A&A 402, 433–442 (2003)
DOI: 10.1051/0004-6361:20030243

Astronomy & Astrophysics

STELIB: A library of stellar spectra at $R \sim 2000$[⋆,⋆⋆]

J.-F. Le Borgne[1], G. Bruzual[2], R. Pelló[1], A. Lançon[3], B. Rocca-Volmerange[4], B. Sanahuja[5], D. Schaerer[1], C. Soubiran[6], and R. Vílchez-Gómez[7]

[1] Laboratoire d'Astrophysique, UMR 5572, Observatoire Midi-Pyrénées, 14 Avenue E. Belin, 31400 Toulouse, France
[2] Centro de Investigaciones de Astronomía, AP 264, 5101-A Mérida, Venezuela
[3] Observatoire de Strasbourg, UMR 7550, 11 rue de l'Université, 67000 Strasbourg, France
[4] Institut d'Astrophysique de Paris, UMR 7095, 98 bis Boulevard Arago, 75014 Paris, France
[5] Departament d'Astronomia i Meteorologia, Universitat de Barcelona, Martí i Franquès 1, 08028 Barcelona, Spain
[6] Observatoire de Bordeaux, UMR 5804, BP 89, 33270 Floirac, France
[7] Departamento de Física, Universidad de Extremadura, Avda. de la Universidad, s/n 10071 Cáceres, Spain

Received 11 September 2002 / Accepted 14 February 2003

Abstract. We present STELIB⋆, a new spectroscopic stellar library, available at `http://webast.ast.obs-mip.fr/stelib`. STELIB consists of an homogeneous library of 249 stellar spectra in the visible range (3200 to 9500 Å), with an intermediate spectral resolution (≲3 Å) and sampling (1 Å). This library includes stars of various spectral types and luminosity classes, spanning a relatively wide range in metallicity. The spectral resolution, wavelength and spectral type coverage of this library represents a substantial improvement over previous libraries used in population synthesis models. The overall absolute photometric uncertainty is 3%.

Key words. atlases – stars: fundamental parameters – galaxies: stellar content.

1. Introduction

Evolutionary population synthesis models that describe the chemical and spectral evolution of stellar systems in detail are fundamental tools in the analysis of observations of both nearby and distant galaxies (e.g. Guiderdoni & Rocca-Volmerange 1987; Buzzoni 1989; Bruzual & Charlot 2003; Fioc & Rocca-Volmerange 1997). They are needed to determine the stellar populations in a variety of systems, spanning a wide range of metallicities, from early type galaxies and spiral bulges to star forming galaxies at different redshifts.

The possibility of building detailed spectro-chemical evolution models of stellar populations using evolutionary synthesis techniques is limited by the lack of comprehensive empirical libraries of stellar spectra, comprising stars with metallicities ranging from well below solar ([Fe/H] from −2 to −1) to above solar ([Fe/H] > 0). Direct inversions of galaxy spectra (Pelat 1997; Boisson et al. 2000) are also handicaped by this shortage. Current synthesis models based on empirical stellar data are mostly restricted to solar metallicity. In the visible range, they are largely based on the spectral atlas of Gunn & Stryker (1983) or the more recent (and not completely independent) atlas of Pickles (1998).

The use of theoretical stellar spectra such as Kurucz' (1992) instead of empirical libraries is a priori preferable, because they can be computed for a dense grid of fundamental parameters (metallicity, gravity, effective temperatures), thus avoiding interpolation errors and calibrations. However, the resulting synthetic spectra do not in general reproduce the spectral features observed in composite stellar populations with the same degree of accuracy as models based solely on observed stellar spectra. Methods to achieve photometric compatibility between models and data have been developed (Lejeune et al. 1997), and extended and homogeneous libraries of theoretical spectra covering the bulk of the HR-diagram and a wide range of metallicities are now available (Lejeune et al. 1998; Westera et al. 2002). While this represents a major improvement, such libraries still suffer from the limited resolution (~20 Å in the optical). The determination of stellar populations in galaxies up to $z \sim 1$ through optical spectroscopy requires spectral

Send offprint requests to: J.-F. Le Borgne,
e-mail: `leborgne@ast.obs-mip.fr`

⋆ Based on observations collected with the Jacobus Kaptein Telescope, (owned and operated jointly by the Particle Physics and Astronomy Research Council of the UK, The Nederlandse Organisatie voor Wetenschappelijk Onderzoek of The Netherlands and the Instituto de Astrofísica de Canarias of Spain and located in the Spanish Observatorio del Roque de Los Muchachos on La Palma which is operated by the Instituto de Astrofísica de Canarias), the 2.3 m telescope of the Australian National University at Siding Spring, Australia, and the VLT-UT1 Antu Telescope (ESO).

⋆⋆ Tables 5 to 10 and A.3 to A.7 are only available in electronic form at `http://www.edpsciences.org`. The Stellar Library STELIB library is also available at the CDS, via anonymous ftp to `cdsarc.u-strasbg.fr (130.79.128.5)` or via `http://cdsweb.u-strasbg.fr/cgi-bin/qcat?J/A+A/402/433`

synthesis capabilities over a broad wavelength range (~3000 Å to ~1 μm). A minimum spectral resolution of a few Å is necessary to obtain constraints on age, metallicity and global stellar kinematics from absorption lines. The libraries presently available with a suitable spectral resolution (1–3 Å) are often limited to a narrow wavelength range (Jones 1997; Cenarro et al. 2001) or are restricted to particular spectral types (Montes et al. 1999).

The main objective of our stellar library STELIB is to provide a homogeneous set of stellar spectra in the visible range (3200 to 9500 Å), with a relatively high spectral resolution ($\lesssim$3 Å) and sampling (1 Å). This library includes stars of most spectral types and luminosity classes and spans a relatively wide range in metallicity. Most of the stars in our sample have measured metallicities.

The outline of the paper is the following. In Sect. 2 we present the observations. Section 3 describes the selection criteria and the overall characteristics of the STELIB sample of stars. The data reduction process is summarized in Sect. 4. Section 5 presents the content of the library STELIB, presently available through the web. In Sect. 6 we show some particular applications of STELIB to population synthesis studies, and we compare the performances of this library to previous results. The conclusions of this paper are given in Sect. 7.

2. Observations

The data were obtained during two runs, one at the 1 m Jacobus Kaptein Telescope (JKT), Roque de los Muchachos Observatory, La Palma, Canary Islands, Spain, between 1994 March 28 and April 4, and a second one at the 2.3 m of the Australian National University at Siding Spring (SSO), Australia, between 1994 December 25 and 31. On JKT, we used the Richardson-Brealey Spectrograph with the 600 lines/mm grating. The detector was a EEV7 1242×1152 CCD with a 22.5 μm pixel. The slit width was 1.5 arcsec. This configuration gives a dispersion of 1.7 Å/pixel and a resolution of about 3 Å *FWHM*. We made use of both blue and red optics. With the blue optics, spectra were alternatively obtained with 2 grating angle settings: 18° giving a wavelength range of 2900 Å–5100 Å on the CCD (useful data start at ~3200 Å because of atmospheric cutoff) and 21° giving the wavelength range 4300 Å–6500 Å. With the red optics the grating angle settings were 24° and 27° for the wavelength ranges 6000 Å–8200 Å and 7600 Å–9900 Å, respectively. To maximize the efficiency, and to improve the calibration, each night was devoted to a single grating angle setting: changing the grating angle was done manually by opening the spectrograph. March 29 was an exception because 2 settings with the red optics were used (see Table 1 for details). Again to save time, the spectrograph was not rotated to align the slit on the paralactic angle, since it should have to be done manually on the telescope for each pointing. This should have no consequence because of the relatively short wavelength range of each individual spectra, the slit width of 1.5 arcsec, and also because we observed as close to the meridian as possible (the slit was set vertical when at meridian). During the JKT run about 1000 spectra were obtained on about 200 stars.

Table 1. JKT observations: grating angle settings.

night 1994	grating angle	wavelength range
March 28	24°	6000 Å–8200 Å
March 29	24° + 27°	6000 Å–8200 Å + 7600 Å–9900 Å
March 30	21°	4300 Å–6500 Å
March 31	18°	3200 Å–5100 Å
April 1	21°	4300 Å–6500 Å
April 2	24°	6000 Å–8200 Å
April 3	27°	7600 Å–9900 Å
April 4	18°	3200 Å–5100 Å

Table 2. SSO 2.3 m spectrograph configurations (see text).

night 1994	config. number	wavelength ranges	
		blue channel	red channel
December 25	1	3500 Å–4500 Å	6470 Å–7550 Å
December 26	2	4475 Å–5550 Å	7500 Å–8570 Å
December 27	3	5510 Å–6550 Å	8530 Å–9650 Å
December 28	1	3500 Å–4500 Å	6470 Å–7550 Å
December 29	2	4475 Å–5550 Å	7500 Å–8570 Å
December 30	3	5510 Å–6550 Å	8530 Å–9650 Å
December 31	1	3500 Å–4500 Å	6470 Å–7550 Å

The spectrograph used at the Siding Spring 2.3 m telescope was the Double Beam Spectrograph. This instrument has two beams split by a dichroic slide. The detectors were 2 1024×1024 CCD's, the blue channel CCD is UV coated. The grating used was also a 600 lines/mm giving a dispersion of 1.1 Å/pixel (15 μm pixels). The slit width was 2 arcsec on the sky. The spectral resolution was less than 3 pixels *FWHM* with good focus, so about 3 Å. The mode "vertical slit on sky" was used. Three configurations were defined:

– Configuration 1: wavelength range on blue channel: 3500–4500 Å; on red channel: 6470–7550 Å.
– Configuration 2: wavelength range on blue channel: 4475–5550 Å; on red channel: 7500–8570 Å.
– Configuration 3: wavelength range on blue channel: 5510–6550 Å; on red channel: 8530–9650 Å.

Table 2 summarizes the configurations used during this run. 36 stars were obtained at Siding Spring. They were selected mainly in the Large Magellanic Cloud or among local metal poor stars, in order to improve the coverage of stellar parameter space. Some Wolf Rayet stars were also observed.

3. Star selection

Most stars were originally selected from the catalogue of Cayrel de Strobel et al. (1992) according to the value of [Fe/H]. Additional samples of 62 and 45 stars were selected to include targets with either near-IR spectra (from Lançon & Rocca-Volmerange 1992) and/or UV data (from IUE) respectively.

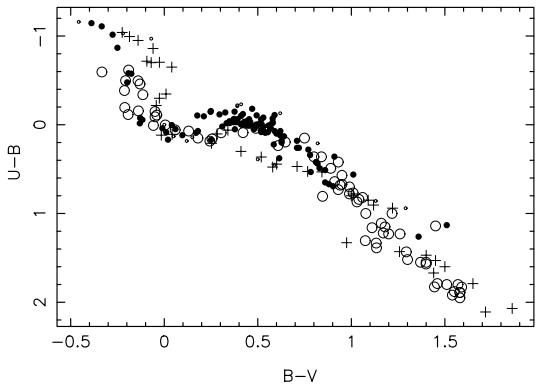

Fig. 1. $U-B$ vs. $B-V$ for the stars in STELIB corrected for interstellar extinction. The different symbols represent different stellar spectral classes: full circles are dwarf main sequence stars (class V), open circles, giants (class III) and plus sign, super-giants of classes I and II. Small circles are used for stars with no spectral class determination.

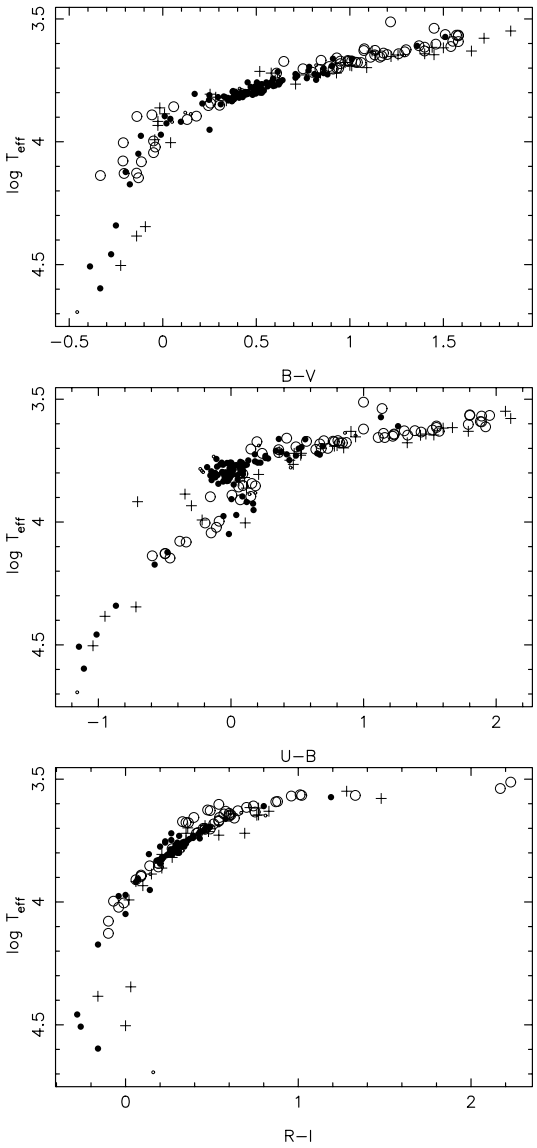

Fig. 2. $T_{\rm eff}$ vs. $B-V$, $U-B$ and $R-I$. The colors are corrected for interstellar extinction. Symbols are the same as in Fig. 1.

The Tables 5 to 10 give the list of the 249 stars included in the library. Most of the atmospheric parameters ($T_{\rm eff}$, log(g), [Fe/H]) listed in Tables 5 to 10 come from the 2 latest editions of the Catalogue of [Fe/H] determinations (Cayrel de Strobel et al. 1997, 2001). This compilation was complemented by accurate $T_{\rm eff}$ listed in Blackwell & Lynas-Gray (1998), di Benedetto (1998) and Alonso et al. (1996, 1999). We have also used the $V-K$ colour index, when available, calibrated into $T_{\rm eff}$ using the formulae of Alonso et al. (1996, 1999). Multiple determinations of atmospheric parameters for the same star were averaged, giving more weight to the most recent ones. Several stars with unknown atmospheric parameters were also part of the ELODIE database (Prugniel & Soubiran 2001). In that case we give the parameters determined by the TGMET method (Katz et al. 1998).

Absolute magnitudes M_v were derived from the Hipparcos parallax and TYCHO2 $V_{\rm T}$ apparent magnitude, transformed into V Johnson band (Høg et al. 2000) and corrected with A_v measured on the spectra. M_v is only given for stars having a relative parallax error lower than 30%. Uncertainties correspond to one σ errors on parallaxes and V magnitudes.

Most of the stars in the library have accurate UBV photometry available from the Lausanne "General Catalogue of Photometric Data" compiled by Mermilliod et al. (1997) and about half of them have R and I photometry. Figure 1 shows the $U-B$ vs. $B-V$ diagram corrected for the interstellar extinction with $A_V/E_{B-V}=3.1$, $E_{U-V}/E_{B-V}=1.59$, $E_{R-V}/E_{B-V}=-0.88$ and $E_{I-V}/E_{B-V}=-1.60$. The relations $T_{\rm eff}$ versus color indices are displayed in Fig. 2. Finally, HR-type diagrams are shown in Fig. 3. In the log(g)/$T_{\rm eff}$ diagram and $M_V/T_{\rm eff}$ diagrams, evolutionary tracks from the Geneva models (Schaller et al. 1992) are displayed for solar metallicity. In the diagram M_V versus $T_{\rm eff}$ and M_V versus $B-V$, M_V are from the Hipparcos catalog (Perryman et al. 1997). Figure 4 shows the distribution of [Fe/H] as a function of $T_{\rm eff}$.

4. Data reduction

The basic data reduction was performed with iraf[1] except for the flux calibration of JKT data which appeared to demand non-standard procedures.

The wavelength calibration was done thanks to the acquisition of arc spectra from a Cu-Ne lamp for the JKT data and from He-Ar, Ar-Ne and Cu-Ar lamps for the SSO data. The typical number of lines used was 30 to 50. The rms of the residuals is of the order of 0.1 Å.

Table 3 gives the list of the standard stars observed at JKT. In average, 18 spectra of standard stars were obtained each night, enough to allow checking for atmospheric extinction. The examination of these spectra revealed strongly varying

[1] IRAF is distributed by the National Optical Astronomy Observatories, USA, which are operated by the Association of Universities for Research in Astronomy, Inc., under cooperative agreement with the National Science Foundation, USA.

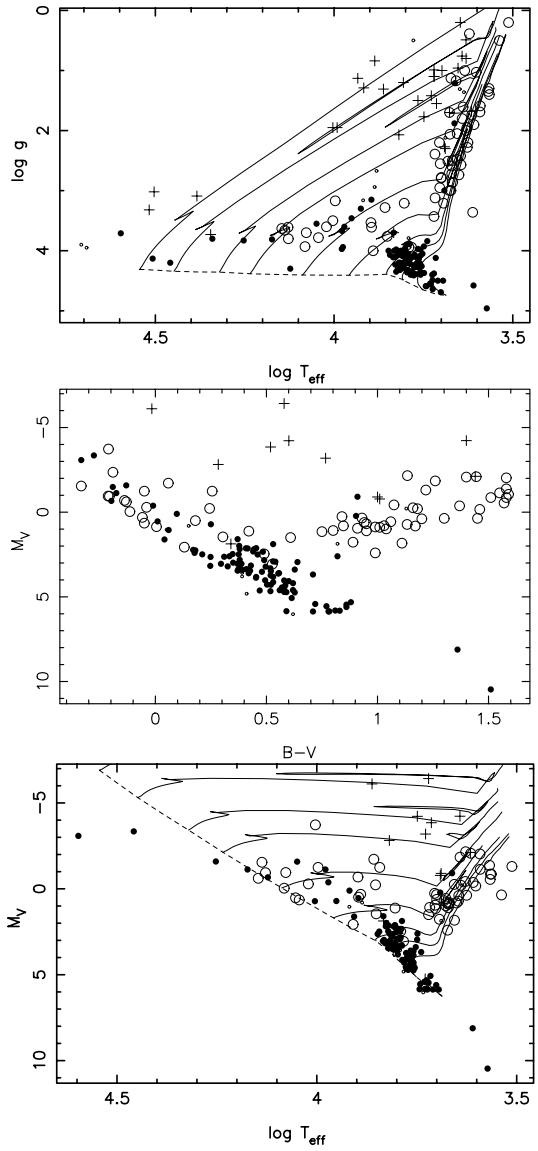

Fig. 3. Log(g) vs. log($T_{\rm eff}$) and HR diagrams. Symbols are the same as in Fig. 1.

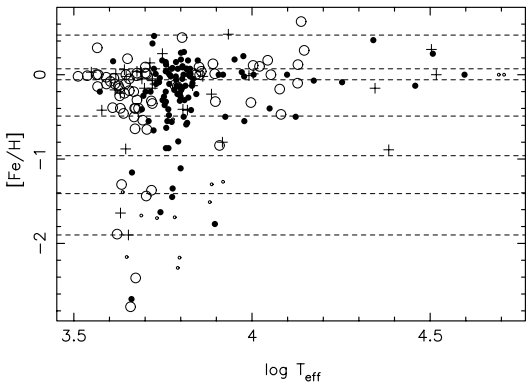

Fig. 4. Metallicity distribution. Symbols are the same as in Fig. 1. Horizontal lines show the limits of the subsets described in Table 11.

Table 3. Standard stars observed at JKT.

star	num. of spectra	rms	reference
HR 2422	19	0.058	Whiteoak (1966)
HR 3454, η Hya	31	0.024	Hamuy et al. (1992), (1994)
HR 4963, θ Vir	29	0.020	Hamuy et al. (1992), (1994), Hayes (1970)
HR 3982, Regulus	27	0.020	Cochran (1981), Hayes (1970)
HR 5511, 109 Vir	17	0.036	Cochran (1981) Johnson (1980)
HR 7001, Vega	11	0.022	Hayes (1985)
HR 7589	15	0.041	Whiteoak (1966)

atmospheric extinction during the observations. Our interpretation is that the strong wind blowing from east was carrying dust from the Sahara desert. But we cannot exclude that it comes from differential atmospheric loss in the JKT narrow slit.

As a consequence, the direct use of the standard stars spectra, with a standard procedure to flux calibrate the spectra was not feasible. We then built a procedure to take into account various factors which affect the atmospheric extinction both in its absolute value and its dependence with wavelength.

The normal atmospheric extinction is modeled by the mean atmospheric extinction curve versus wavelength and the airmass at time of observation. The "abnormal" extinction, possibly due to dust, is likely to change rapidly during one night. We calibrated this effect by using any observed star as a photometric standard star. The *UBVRI* photometry of most of our program stars are available in the Lausanne database (`http://obswww.unige.ch/gcpd/gcpd.html`) (Mermilliod et al. 1997). However to do this, it has been necessary to take the variation of seeing into account. The seeing, measured on each spectrum from the profile of the star image along the slit, appeared to change significantly during the nights, typically between 0.6″ and 1.5″. The light lost outside the slit differs as the seeing varies. To model it, we took into account the stellar profile and the slit width. The detailed modelling process was performed individually for each star. This operation gives an absolute mean value over the wavelength for a given grating angle setting to scale the spectra. Then, the observations of spectrophotometric standard stars were used to analyse the wavelength dependence of the additionnal extinction.

Figures 5 and 6 show the comparison of the calibrated standard stars spectra with published SED. The spectrum of Vega (Fig. 5) was obtained only in the shortest wavelenth setting because of its brightness. The comparison for the other standards are shown in Fig. 6. The rms of difference between calibrated spectra of standard stars and published spectra, expressed in magnitude, are given in Table 3. They are computed avoiding the strong absorption lines where the difference of wavelength sampling introduces large dispersions.These rms are between 0.02 and 0.04 mag. An exception is HR 2422 for which the rms is 0.058.

The SSO spectra were reduced using the standard procedures for flux calibration. Table 4 lists the standard stars used. Two target stars and one standard star observed in this run were

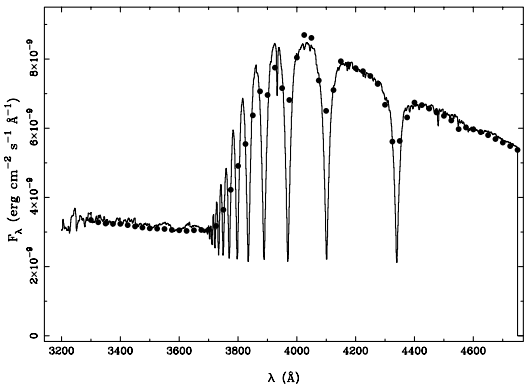

Fig. 5. Comparison of Vega spectrum in the UV with published SED (filled circles).

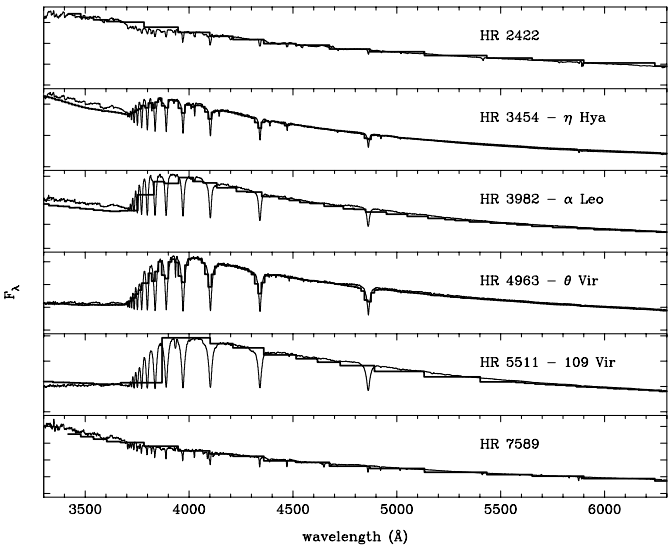

Fig. 6. Comparison of calibrated standard stars spectra observed at JKT with published SED (bold curve).

also observed at JKT. We used these stars as an additional check on the reliability of the complex flux calibration procedure applied to JKT data. A good agreement was obtained between the two independent set of spectra. Figure 7 shows the comparison of the calibrated standard stars spectra with published SED. As for the JKT standard stars, the rms of difference between calibrated spectra of standard stars and published spectra, are given in Table 4. They are also computed avoiding the strong absorption lines. The rms have similar values between 0.02 and 0.04 mag. One standard star, η Hya, has been observed during both runs. The rms of the difference is 0.031 mag, of the same order than the rms of the difference between observed and published spectra. Thus, we can consider that 0.03 mag is the typical absolute photometric uncertainty of the library. In addition, the detailed comparison between the synthetic photometry derived from the STELIB library and the Lausanne database is presented and discused in Appendix A. Tables A.3 to A.6 provide with the *UVBRI* synthetic photometry for STELIB stars.

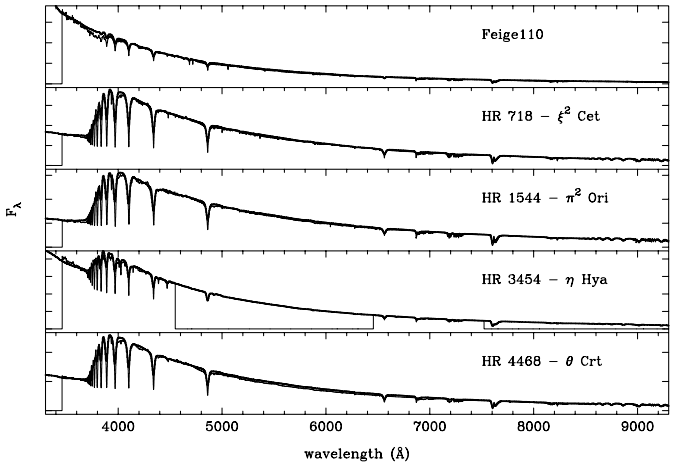

Fig. 7. Comparison of calibrated standard stars spectra observed at SSO 2.3 m with published SED (bold curve).

Table 4. Standard stars observed at SSO.

star	rms (mags)	reference
HR 3454, η Hya	0.024	Hamuy et al. (1992, 1994)
HR 718, ξ^2 Cet	0.027	Hamuy et al. (1992, 1994)
Feige 110	0.043	Oke (1990), Hamuy et al. (1992, 1994)
HR 4468, θ Crt	0.031	Hamuy et al. (1992, 1994)
HR 1544, π^2 Ori	0.024	Hamuy et al. (1992, 1994)

5. The library

Once calibrated, the spectra in the 4 (JKT) or 6 (SSO) settings of the program stars were combined by averaging the overlapping pixels. This results in 257 stellar spectra in fits format resampled with a step of 1 Å per pixel. The library is available in two different forms: the "raw" data, including the combined spectra as coming out of the calibration process, and the data corrected for interstellar reddening using the empirical extinction function of Cardelli et al. (1989). As an additional check, we have compared the reddening corrected spectra (using the extintion values from the literature) to the equivalent ones in the Kurucz atlas (same spectral type and metallicity). In most cases (~80%), the agreement between the two spectra is excellent. In case of discrepancy (~20% of the sample), the extintion values used and quoted in the tables are those allowing to match our corrected spectra to Kurucz. These discrepant objects are clearly identifyed on the web site.

6. Synthetic spectra of stellar populations

Templates of stellar populations have been built from the dereddened library. At this stage, the wavelength scale was corrected for radial velocity. For some stars, data are missing in limited wavelength ranges: for these, we filled the gaps using spectra of stars of similar or close spectral type. The final spectra are useful from 3200 to 9300 Å because spectra become noisy from 9300 Å to 9850 Å. In this way, we built several subsets of the atlas with different [Fe/H] ranges (Table 11). These subsets

Table 11. Subsets of stars according to their metallicity.

	[Fe/H] range	number of stars
	<−1.90	6
	[−1.90, −1.41]	12
sub-solar	[−1.40, −0.96]	6
	[−0.95, −0.49]	23
	[−0.48, −0.06]	69
solar	[−0.06, +0.07]	84
above	[+0.08, +0.47]	38
solar	>+0.47	4

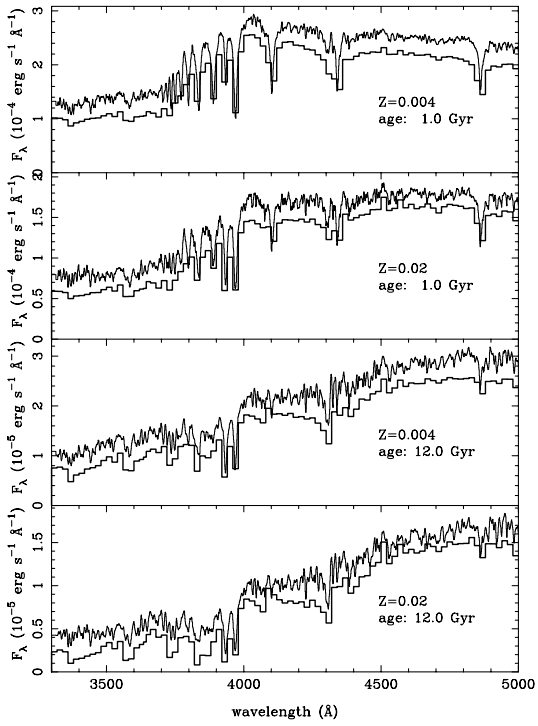

Fig. 8. Synthetic spectra built with STELIB compared to synthetic spectra obtained with Kurucz spectra using GISSEL02. SSP, wavelength range 3300 Å to 5000 Å, $Z = 0.02$ (solar metallicity) and $Z = 0.004$, from 1 Gyr to 12 Gyr. The Kurucz spectra are shifted downward by 10% of the scale for clarity.

include a total of 242 star templates which are also available on the web site.

6.1. Comparison with Kurucz spectra

In order to compare with the previous results, and to show the capabilities of this new library, we have built galaxy models with the STELIB library in the apropriate subset, using the new galaxy evolutionary code GISSEL02 (Bruzual & Charlot 2003). The evolution of a single stellar population of solar metallicity ($Z = 0.02$) is given in Figs. 8 and 9, for ages of the stellar population ranging from 1 to 12 Gyr. A comparison with the same models obtained with the synthetic stellar spectra from Kurucz is also shown to emphasize the gain in spectral resolution.

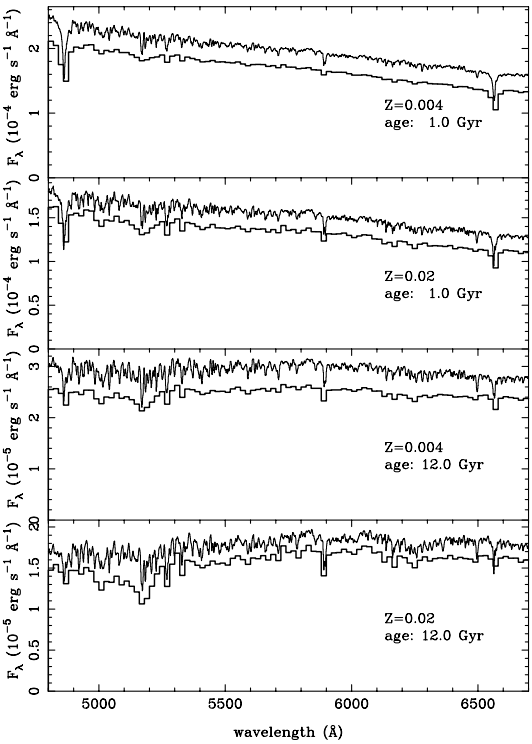

Fig. 9. Synthetic spectra built with STELIB compared to synthetic spectra obtained with Kurucz spectra using GISSEL02. SSP, wavelength range 4800 Å to 7000 Å, $Z = 0.02$ (solar metallicity) and $Z = 0.004$, from 1 Gyr to 12 Gyr. The Kurucz spectra are shifted downward by 10% of the scale for clarity.

6.2. Modeling observed spectra of galaxies

An important application of STELIB is to reproduce in details the spectral features observed in galaxies at $z \lesssim 1$. As an example, we present here the modeling of spectra of galaxies belonging to the cluster AC 114 (more officially named ACO S 1077, Abell et al. 1989) at a redshift of $z = 0.312$, and some foreground galaxies in the same field. These spectra were obtained with the spectrograph FORS1 on VLT unit 1 Antu, on october 5, 1999. The main objective of the run was the determination of the redshift of background lensed galaxies, but spectra of cluster galaxies were also obtained in the remaining slits. The grism used was G300V, with a wavelength coverage between ~4000 Å and ~8600 Å, and a wavelength resolution of $R = 500$ for the 1″ slit width used which correspond to a resolution of ~7 Å at rest frame of the cluster. Details of the observation conditions and data reduction can be found in Campusano et al. (2001).

A simple best fit procedure has been used to determine the spectral type of each galaxy, acording to its spectral features (see Table 12). We have chosen to display galaxies of different types, from E to irregulars, with good S/N ratio. The models correspond to the evolution with time of a Single Stellar Population (SSP) built with the STELIB library for solar metallicity, assuming Kroupa (2001) IMF. The comparison between observed and modeled spectra is shown in Fig. 10. The best model was chosen among SEDs computed at 11 different ages from 100 Myr to 12 Gyr. The gain in spectral resolution is clear,

Table 12. List of modeled galaxy spectra in the field of AC 114.

USNO	ident.in Fig. 10	RA(2000)	DEC(2000)	exposure time	redshift	spectral type	age of model
U0525_44063178	a	22:59:00.61	−34:46:20.8	2700 s	0.1418	elliptical	12 Gyr
	b	22:58:37.19	−34:49:27.8	5400 s	0.2605	irregular	500 Myr
U0525_44063148	c	22:58:43.07	−34:48:48.1	5400 s	0.2999	irregular	500 Myr
	d	22:58:56.93	−34:47:57.4	2700 s	0.3113	spiral	1 Gyr
	e	22:58:46.51	−34:49:09.6	4218 s	0.3139	elliptical	12 Gyr
U0525_44062505	f	22:58:37.67	−34:49:24.8	4218 s	0.3147	elliptical	12 Gyr
U0525_44063303	g	22:58:44.48	−34:49:11.3	4218 s	0.3163	elliptical	12 Gyr
U0525_44063178	h	22:58:43.35	−34:49:36.5	5400 s	0.3207	irregular	500 Myr

with obvious applications in stellar population synthesis modelling. In particular, STELIB allows to determine the stellar populations using the strengths of a large number of absorption lines, due to the wide spectral coverage, and thus to improve the emission-line measurements in star-forming galaxies and AGNs.

7. Conclusions

We have presented the main characteristics of the public stellar library STELIB, available on the web site `http://webast.ast.obs-mip.fr/stelib`. The main improvements with respect to other previous libraries are:

1. The homogeneous and relatively large spectral coverage, from 3200 to 9500 Å.
2. The high spectral resolution and sampling for such a spectral coverage.
3. The wide metallicity range, although the present sample still needs some completion for extreme metallicities.

We have presented some qualitative examples on the possible use of STELIB for population synthesis and evolutionary models of galaxies. Fundamental Plane studies of high redshift galaxies could be another possible application for STELIB (Treu et al. 2001). In general, STELIB should be a useful tool for detailed studies of galaxies at $z \lesssim 1$, based on optical spectra at intermediate resolution.

Acknowledgements. We would like to thanks J.-C. Mermilliod who provided us a file extracted from the Lausanne photometric database. Many thanks to Stéphane Charlot for for a careful reading of the manuscript. This research has made use of the SIMBAD database, operated at CDS, Strasbourg, France. We are grateful to the help of the staff of Roque de los Muchachos Observatory at La Palma and of Siding Spring Observatory in Australia, where these observations were conducted. Some examples shown in this paper come from observations collected at the European Southern Observatory, Chile (ESO No. 64.O-0439). Part of this work was supported by the French *Centre National de la Recherche Scientifique*, and by the French *Programme National Galaxies* (PNG). G. Bruzual acknowledges ample support from the Venezuelan Ministerio de Ciencia y Tecnología and FONACIT. G. Bruzual also thanks Observatoire Midi-Pyrénées and the MENRT for their support during stays in Toulouse.

Table A.1. Characteristics of filters used in Appendix A: the effective wavelength $\lambda_{\rm eff}$ and the band width.

Filter	$\lambda_{\rm eff}$ [Å]	width [Å]
U	3594	377
B	4462	742
V	5554	736
R	6939	1507
I	8548	1307
$I_{\rm Cousins}$	8060	924

Table A.2. Dispersion values in the comparison between synthetic magnitudes and photoelectric photometry from the Lausanne database.

quantity	rms	quantity	rms
ΔU	0.145	$\Delta U-B$	0.156
ΔB	0.044	$\Delta B-V$	0.083
ΔV	0.072	$\Delta V-R$	0.135
ΔR	0.172	$\Delta R-I$	0.177
ΔI	0.249		

Appendix A: Synthetic photometry and photometric reliability of STELIB

We present in this section a detailed comparison between the synthetic photometry derived for the STELIB library and the Lausanne database (Mermilliod et al. 1997). Magnitudes for STELIB stars have been obtained using the flux calibrated spectra without any correction for dereddening or radial velocity. The photometric bands are *UBVRI*, with filter transmissions as close as possible to the Johnson filters commonly used in the Lausanne database. Table A.1 summarizes the characteristics of the different filters.

Tables A.3 to A.6 provide with the *UVBRI* synthetic photometry for most of STELIB stars, together with the photoelectric photometry coming from the Lausanne database. Stars known to be variable or for which the spectrum is incomplete in a given filter have been discarded from this analysis. Almost all stars in this library have *UBV* Johnson magnitudes available, whereas *R* and *I* magnitudes are available only for 70% of the whole sample. In addition, magnitudes in the *R* and *I* bands are given either in the Johnson system or in the Eggen or Cousins systems. The later are identified by a comment in the last column of Tables A.3 to A.6. When a filter band is missing

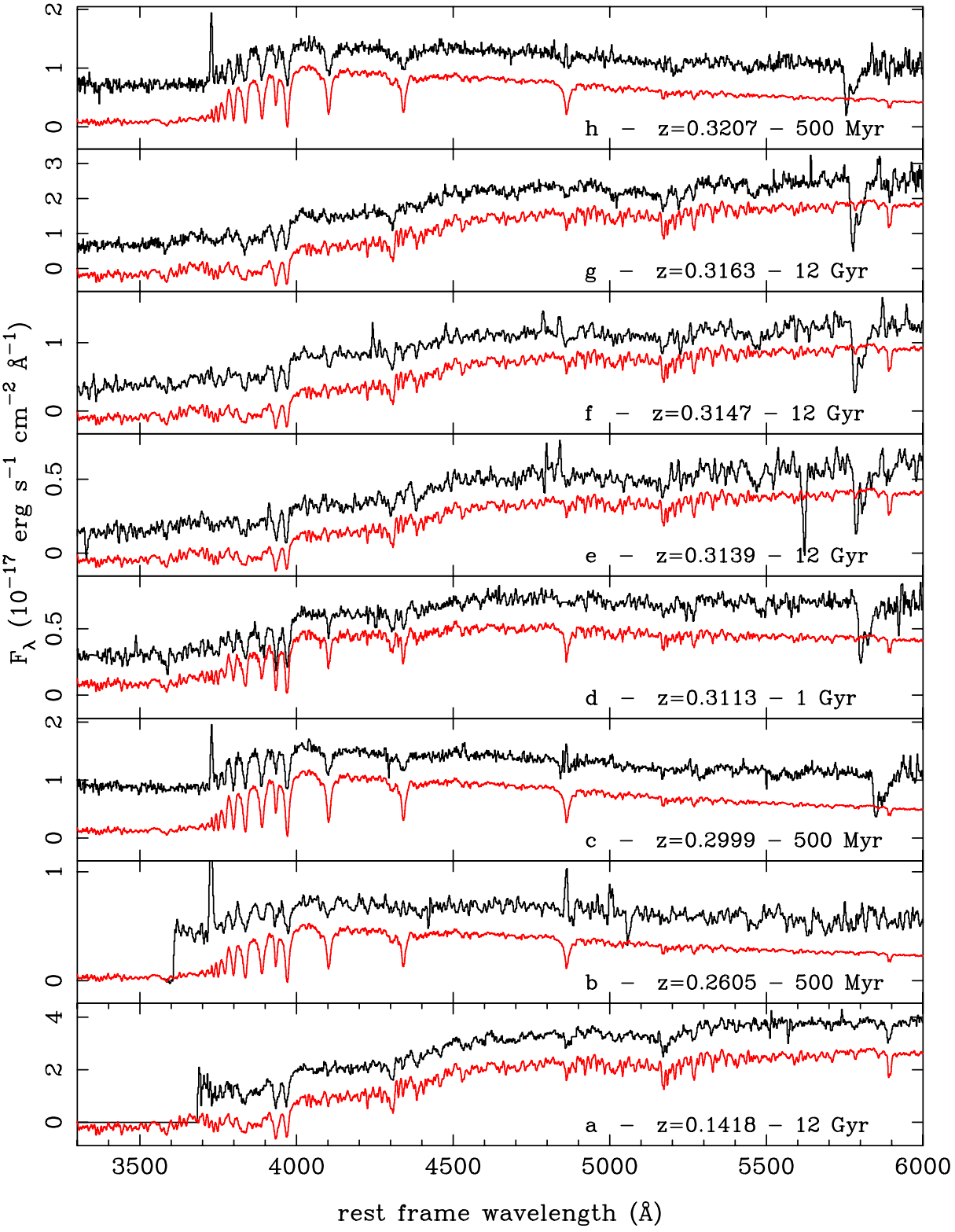

Fig. 10. Comparison of galaxy spectra, in and foreground of the cluster of galaxies AC 114, with solar metallicity SSP synthetic spectra. See Table 12 for identification. The observed spectra are not corrected for atmospheric molecular bands (the main one appears at about 5800 Å for $z \sim 0.3$ galaxies). The observed spectra appear as a black line, and the model as a grey line. The model spectra are shifted downward by 20% of the scale for clarity. The legends in the figure give the observed redshift of the galaxies and the age of the models. The contribution of emission lines in the Balmer series is visible on observed spectra b, c and h.

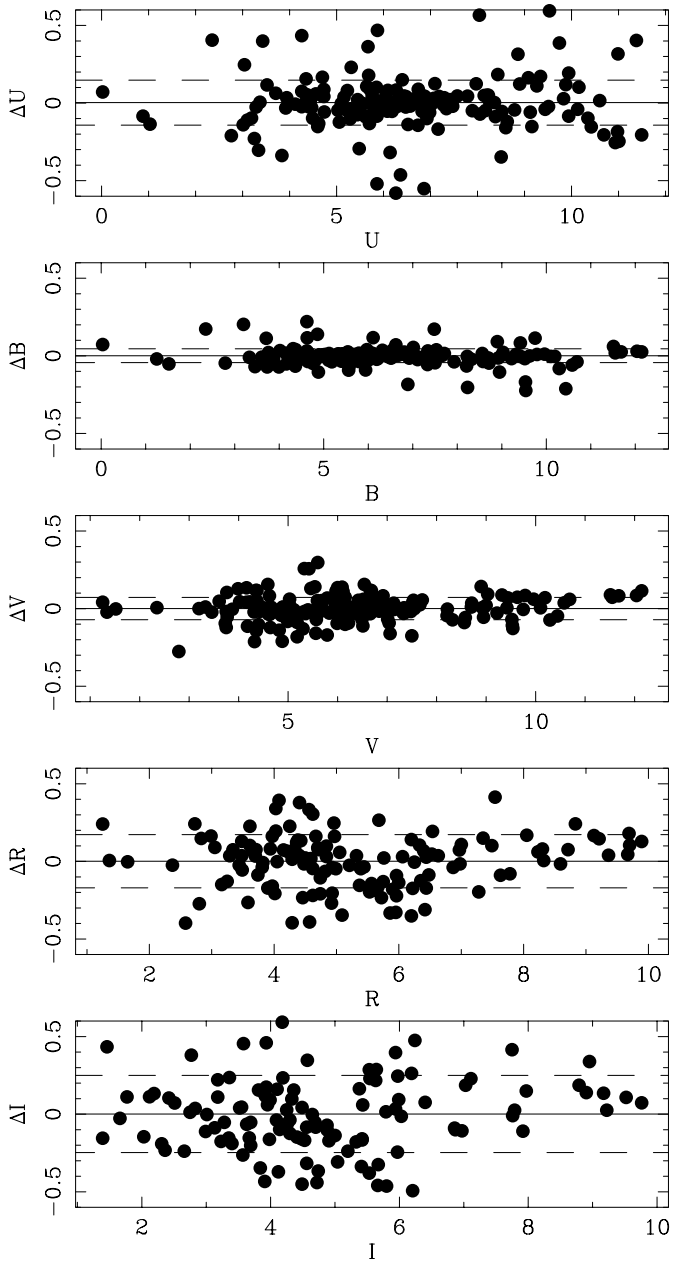

Fig. A.1. Residuals of the comparison between synthetic photometry and published photoelectric photometry: *UBVRI* magnitude residuals versus Johnson magnitudes in the Lausanne database. Dashed lines correspond to 1 σ rms.

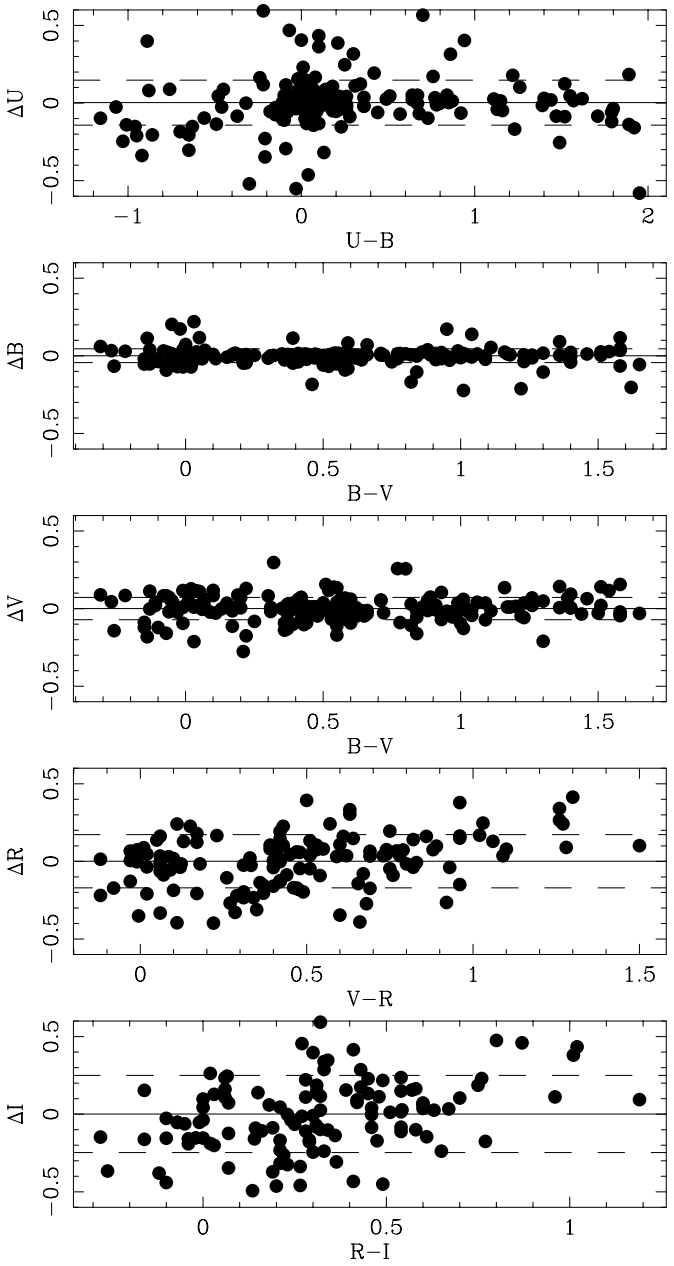

Fig. A.2. Residuals of the comparison between synthetic photometry and published photoelectric photometry: *UBVRI* magnitude residuals versus Johnson colors in the Lausanne database. Dashed lines correspond to 1 σ rms.

in the STELIB spectra, the corresponding magnitude is given by "-" in the tables. A small extrapolation up to ~100 Å is allowed in *U* and *I* when needed, towards the blue and the red edges of the filters. The following caveats apply in the comparison of photoelectric with synthetic magnitudes derived from our spectra:

- The effective filter transmissions in the different bands could be different between the photoelectric and the synthetic magnitudes.
- The transmission of the Johnson *U* band has been set to zero in our calculations for wavelengths shorter than 3200 Å, which corresponds to the blue limit of the STELIB spectra.
- Although the majority of stars in the Lausanne database are given in the Johnson system, STELIB spectra do not cover completely the standard *I* band. Thus, the effective transmission in the *I* band has been adapted to the red limit of our spectra in wavelength. When spectra extend up to ~9800 Å, we use the broadest and redest version of the *I* band filter, identified by *I* in Table A.1, which is closer (although not identical) to a true Johnson filter. For spectra with red wavelegth limits bluer than ~9800 Å, we used the *I* Cousins filter instead, identified by $I_{\rm Cousins}$ in Table A.1. These stars are identified by an asterisk in Tables A.3 to A.6.

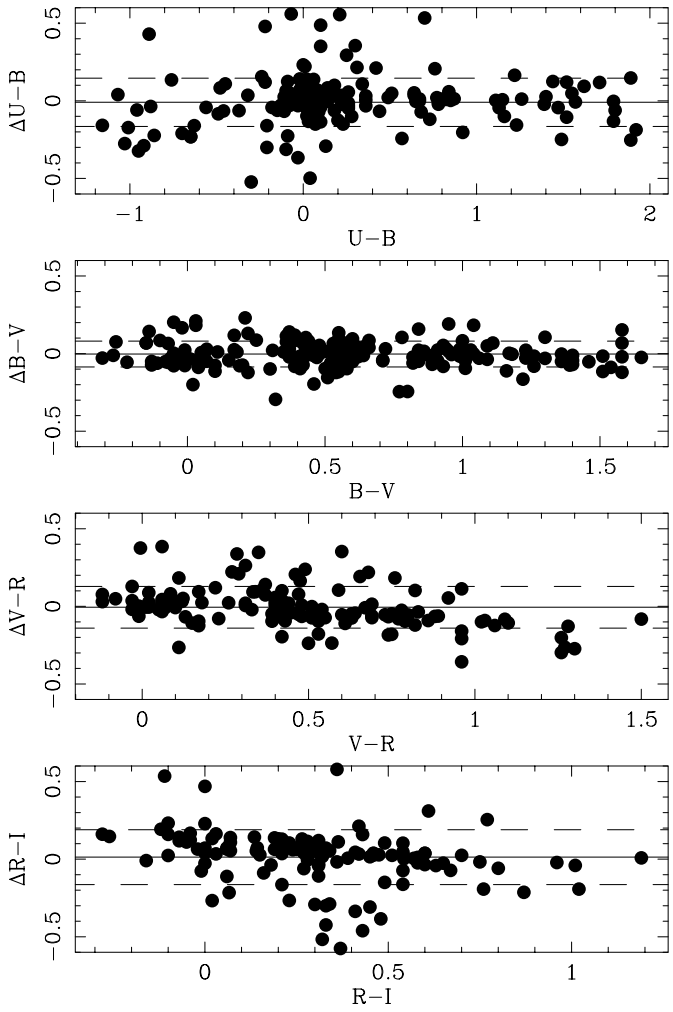

Fig. A.3. Residuals of the comparison between synthetic photometry and published photoelectric photometry: color residuals versus Johnson colors in the Lausanne database. Dashed lines correspond to 1 σ rms.

Figures A.1 to A.3 display the residuals of the comparison between synthetic photometry and the published Lausanne database. Table A.2 summarizes the dispersion values obtained in the different filters and colors. As expected, the smallest dispersions correspond to the *B* and *V* magnitudes and $B-V$ colors, for which we have the highest degree of confidence in the correspondance between filter bands. For these 2 filters, the rms dispersion is quite consistent with the photometric accuracy derived from standard stars. The dispersion is much higher in the *I* band, as expected taking into account the inhomogeneities both in the photometric systems and the wavelegth coverage for the different objects. The situation in the *U* and *R* bands are intermediate. The wavelegth coverage could be responsible for the dispersion in *U*, (where the photometric systems are more consistent than in *I*), whereas the culprit in *R* is more likely the photometric system, but this point is difficult to assess. According to Figs. A.1 to A.3, there is no obvious color trend in the residuals neither in magnitude nor in color, except for the $R-I$ and maybe in $V-R$ in Fig. A.3. This color trend is due to a residual difference between the filters used to compute synthetic magnitudes and the true Johnson filter. On the other hand, the relatively small dispersion in the $R-I$ residuals as compared to the corresponding dispersion in *R* and *I* magnitudes (Fig. A.3) indicates that the two photometric systems used are both internally consistent, but different from each other.

References

Abell, G. O., Corwin, H. G. Jr, & Olowin, R. P. 1989, ApJS, 70, 1
Alonso, A., Arribas, S., & Martínez-Roger, C. 1996, A&AS, 117, 227
Alonso, A., Arribas, S., & Martínez-Roger, C. 1999, A&AS, 140, 261
Blackwell, D. E., & Lynas-Gray, A. E. 1998, A&AS, 129, 505
Boisson, C., Joly, M., Moultaka, J., Pelat, D., & Serote Roos, M. 2000, A&A, 357, 850
Bruzual, G., & Charlot, S. 2003, in preparation
Buzzoni, A. 1989, ApJS, 71, 817
Campusano, L. E., Pello, R., Kneib, J.-P., Le Borgne, J.-F., et al. 2001, A&A, 378, 394
Cardelli, J. A., Clayton, G. C., & Mathis, J. S. 1989, ApJ, 345, 245
Cochran, A. L. 1981, ApJS, 45, 83
Cayrel de Strobel, G., Hauck, B., Francois, P., et al. 1992, A&AS, 95, 273
Cayrel de Strobel, G., Soubiran, C., Friel, E. D., Ralite, N., & Francois, P. 1997, A&AS, 124, 299
Cayrel de Strobel, G., Soubiran, C., & Ralite, N. 2001, A&A, 373, 159
Cenarro, A. J., Cardiel, N., Gorgas, J., et al. 2001, MNRAS, 326, 959
di Benedetto, G. P. 1998, A&A, 339, 858
Fioc, M., & Rocca-Volmerange, B. 1997, A&A, 326, 950
Guiderdoni, B., & Rocca-Volmerange, B. 1987, A&A, 186, 1
Gunn, J. E., & Stryker, L. L. 1983, ApJS, 52, 121
Hamuy, M., Walker, A. R., Suntzeff, N. B., et al. 1992, PASP, 104, 533
Hamuy, M., Suntzeff, N. B., Heathcote, S. R., et al. 1994, PASP, 106, 566
Hayes, D. S. 1970, ApJ, 159, 165
Hayes, D. S. 1985, in Calibration of fundamental stellar quantities; Proceedings of the Symposium, Como, Italy, May 24-29, 1984 (Dordrecht: D. Reidel Publishing Co.), 225
Høg, E., Fabricius, C., Makarov, V. V., et al. 2000, A&A, 355, L27
Johnson, H. L. 1980, Rev. Mex. Astron. Astrofis., 5, 25
Jones, L. A. 1997, Ph.D. Thesis, University of North Carolina at Chapel Hill
Katz, D., Soubiran, C., Cayrel, R., Adda, M., & Cautain, R. 1998, A&A, 338, 151
Kurucz, R. L. 1992, IAU Symp. 149: The Stellar populations of Galaxies, ed. B. Barbuy, & A. Renzini (Kluwer Academic Publishers), 225
Kroupa, P. 2001, MNRAS, 322, 231
Lançon, A., & Rocca-Volmerange, B. 1992, A&AS, 96, 593
Lejeune, T., Cuisinier, F., & Buser, R. 1997, A&AS, 125, 246
Lejeune, T., Cuisinier, F., & Buser, R. 1998, A&AS, 130, 75
Mermilliod, J.-C., Mermilliod, M., & Hauck, B. 1997, A&AS, 124, 349
Montes, D., Ramsey, L. W., & Welty, A. D. 1999, ApJS, 123, 283
Oke, J. B. 1990, AJ, 99, 1621
Pelat, D. 1997, MNRAS, 284, 365
Perryman, M. A. C., Lindegren, L., Kovalevsky, J., et al. 1997, A&A, 323, L49
Pickles, A. J. 1998, PASP, 110, 863
Prugniel, P., & Soubiran, C. 2001, A&A, 369, 1048
Schaller, G., Schaerer, D., Meynet, G., & Maeder, A. 1992, A&AS, 96, 269
Treu, T., Stiavelli, M., Bertin, G., Casertano, S., & Møller, P. 2001, MNRAS, 326, 237
Westera, P., Lejeune, T., Buser, R., Cuisinier, F., & Bruzual, G. 2002, A&A, 381, 524
Whiteoak, J. B. 1966, ApJ, 144, 305